OPEN ACCESS
Applied Physics Express 13, 017006 (2020)
https://doi.org/10.7567/1882-0786/ab626e

LETTER

First-principles study of crystalline Nd–Fe alloys

Yuta Ainai[1], Yasutomi Tatetsu[1,2], Asako Terasawa[1], and Yoshihiro Gohda[1*]

[1]Department of Materials Science and Engineering, Tokyo Institute of Technology, Yokohama 226-8502, Japan
[2]University Center for Liberal Arts Education, Meio University, Nago 905-8585, Japan

*E-mail: gohda.y.ab@m.titech.ac.jp

Received October 23, 2019; revised November 28, 2019; accepted December 16, 2019; published online January 3, 2020

We report the crystal structure of Nd–Fe alloys as candidates for grain-boundary phases in Nd–Fe–B sintered magnets. We find that the crystal structure of the fluorite Nd–Fe alloys is stable for a wide composition range. We also demonstrate that solid solution of Ga is effective in stabilizing the fluorite crystal structure of Nd–Fe alloys, which is consistent with experimental observations reporting crystalline Nd–Fe alloys at the grain boundaries of Ga-added Nd–Fe–B permanent magnets. © 2020 The Japan Society of Applied Physics

Nd–Fe–B sintered magnets are used in a wide range of industry products such as wind-turbine generators and the electric-vehicle motors, due to their high maximum energy products.[1–8] Nevertheless, it is problematic that the coercivity of Nd–Fe–B sintered magnets decreases significantly at high temperatures showing typically only 0.2 T at around 500 K. The key to improving the coercivity of Nd–Fe–B sintered magnets lies not only in the physical property of the main phase, $Nd_2Fe_{14}B$, but also in microstructures, e.g. the chemical composition, the magnetism and the thickness of subphases.[9–17] In particular, among the subphases in Nd–Fe–B sintered magnets, grain-boundary (GB) phases consisting mainly of Nd and Fe have impact on achieving the high coercivity. This is attributed to the fact that the electronic states of microstructure interfaces between the main phase and GB phases are responsible for the pinning effect to prevent the magnetization reversal caused by thermal fluctuation.[18,19] Recent investigations have demonstrated that doping of metallic elements such as Al, Co, Cu, and Ga greatly modifies the microstructure including the GB phase improving the coercivity.[20–23] In this sense, the atomic configurations and the magnetism of the GB phase is of significant importance.

It has been reported the chemical composition, the structure, and the magnetic state of GB phases strongly depend on the surface index of the main phase grains.[23,24] In particular, the GB phase facing at the (001) surface of the main phase is crystalline, containing approximately 60–70 at% of Nd and nonmagnetic at room temperature.[23] Even though the structure of this crystalline Nd–Fe GB phase has been reported as the fcc type for Ga-added Nd–Fe–B permanent magnets from the nanobeam-electron-diffraction pattern and the fast-Fourier-transform pattern of the high angle annular dark field images of scanning transmission electron microscope,[24] more details of the structure are yet to be identified.

In this letter, we systematically investigate the structure for Nd–Fe alloys as fcc-type GB phases by first-principles calculations. Among the tested crystal structures of $Nd_{0.67}Fe_{0.33}$, fluorite, half-Heusler, cuprite, fcc, and quasi-sphalerite, the fluorite structure is found to be most stable. Furthermore, we find that the crystal structure of the fluorite Nd_xFe_{1-x} is stable for a wide composition range of approximately $0.6 < x \leqslant 1$, even though the structural phase transition into another phase is expected for large x. The fluorite crystal structure for $0.67 \leqslant x \leqslant 1$ has negligibly small distortions with the Fe-vacancy formation. For $x < 0.67$ having structures with the substitution of Nd at the 8c sites by Fe, the distortion of the fluorite structure becomes larger as x becomes smaller. The formation energy for this phase is always positive, which means that the separated pure phases of double hcp (dhcp) Nd and bcc Fe are more stable at the zero temperature. To stabilize the binary fluorite alloys, the entropy of mixing is necessary as the finite-temperature effect. In addition, we examine the effect of a third element for Al, Cu, Co, and Ga with its composition y up to approximately 20 at%. We identify that the ternary Nd–Fe–Ga alloy with the fluorite structure is more stable than the corresponding Nd–Fe binary structure, where Nd–Fe–Ga can even have negative formation energies. In this case, Ga atoms preferably occupy Fe sites.

Our first-principles calculations of Nd_xFe_{1-x} and $Nd_{0.67}Fe_{0.33-y}M_y$ (M = Al, Co, Cu, and Ga) alloys are based on density function theory using pseudopotentials and pseudo-atomic-orbital basis functions as implemented in the OpenMX code.[25] In all calculations, the Perdew–Burke–Ernzerhof exchange-correlation functional[26] within the generalized-gradient approximation was used. As basis sets, $s2p2d2$ configurations were adopted for Nd, Fe, Al, Co, Cu, and Ga with cutoff radii of 8.0, 6.0, 7.0, 6.0, 6.0, and 7.0 Bohr, respectively. Semicore orbitals of $3s$ and $3p$ in Fe, Al, Cu, Co, and Ga as well as $5s$ and $5p$ in Nd were treated as valence electrons. An open-core pseudopotential was used for Nd atoms, where $4f$ electrons were treated as spin-polarized core electrons. As for convergence criteria, the maximum force on each atom and the total-energy variation are 10^{-3} Hartree/Bohr and 10^{-5} Hartree, respectively. Collinear spin structures neglecting the spin–orbit coupling of the valence electrons are considered with the energy cutoff of 500 Ry and the k-point grid of $5 \times 5 \times 5$ for the $2 \times 2 \times 2$ cubic unit cell. The initial spin configuration has the antiparallel structure between Nd and Fe, while the parallel configuration is set within Fe and Nd, respectively. We checked that the structural stability is hardly affected by magnetic configurations.

The internal coordinates of the cubic structures except the trivial fcc random alloy for $Nd_{0.67}Fe_{0.33}$ alloys are listed in Table I. Varied compositions in Nd_xFe_{1-x} and $Nd_{0.67}Fe_{0.33-y}M_y$ alloys were examined using the $2 \times 2 \times 2$ supercell. The variation of the composition was examined both by the substitution of atoms, e.g. the substitution of Fe by Nd, and by the formation of vacancies, where energetically more stable crystalline structures were adopted. The special quasirandom structure (SQS) method[27] was adopted to

Table I. Wyckoff positions for Nd and Fe of Nd–Fe alloys with the composition of $Nd_{0.67}Fe_{0.33}$. The number in the labels represents the multiplicity.

Structure	Element	Label	x	y	z
Cuprite	Fe	2a	0.25	0.25	0.25
	Nd	4b	0	0	0
Fluorite	Fe	4a	0	0	0
	Nd	8c	0.25	0.25	0.25
Half-Heusler	Fe	4a	0	0	0
	Nd	4b	0.5	0.5	0.5
	Nd	4c	0.25	0.25	0.25
Sphalerite	Fe	4c	0.25	0.25	0.25
	Nd	4a	0	0	0

determine atomic configurations that are most random within the supercell. For all the examined systems, lattice parameters and atomic positions were relaxed simultaneously. The formation energy E_{form} for $Nd_xFe_{1-x-y}M_y$ is evaluated relative to separated single phases with the most stable crystal structures as

$$E_{\text{form}} = E_{Nd_xFe_{1-x-y}M_y} - [x\mu_{Nd} + (1-x-y)\mu_{Fe} + y\mu_M],$$

where $E_{Nd_xFe_{1-x-y}M_y}$ is the total energy of the $Nd_xFe_{1-x-y}M_y$ alloy per atom and μ_{Nd}, μ_{Fe}, and μ_M are the chemical potentials of dhcp Nd, bcc Fe, and M in the most stable phases, respectively.

First, we discuss the energetic stability of Nd–Fe alloys with the composition of $Nd_{0.67}Fe_{0.33}$ for the crystal structures of fluorite, half-Heusler, cuprite, fcc, and quasi-sphalerite. The quasi-sphalerite structure is prepared by forming vacancies for half of the 4c sites of the sphalerite by the SQS method. The four structures except for fcc have the fcc sublattice either with Nd or Fe atoms, while the fcc structure is constructed as the random alloy by using the SQS method. The fluorite, half-Heusler, and cuprite structures are stable, while the fcc and quasi-sphalerite structures are found to be unstable. Figure 1 shows the optimized crystal structures and the corresponding formation energies for $Nd_{0.67}Fe_{0.33}$. We have found that all the three structures with this composition kept its initial structure exactly after optimization. Furthermore, it is clearly seen that the fluorite structure is most stable without structural distortions. We argue that the best candidate for the fcc-type GB phase experimentally observed[23,24] is the fluorite structure, where further support for this argument will be provided in the following discussions. It should be noted that the formation energy for this phase is positive. It means that the separated pure phases of dhcp Nd and bcc Fe are more stable at the zero temperature, while the entropy of mixing can enhance the formation of the fluorite alloys at finite-temperature.

Next, we examined the effect of the composition variation from $x = 0.67$ for the fluorite Nd_xFe_{1-x} alloys. To increase the composition parameter x, vacancies are formed by removing Fe atoms or Fe atoms are substituted with Nd atoms. We identified in this case that the fluorite structure is obtained with the Fe-vacancy formation at the 4a site. Structural distortions of the fluorite crystal structure with increasing x are found to be negligibly small in all the cases up to $x = 1$, e.g. for $x = 0.8$ (Fig. 2). As also seen in Fig. 2, the formation energy increases as x increases from 0.67. Note

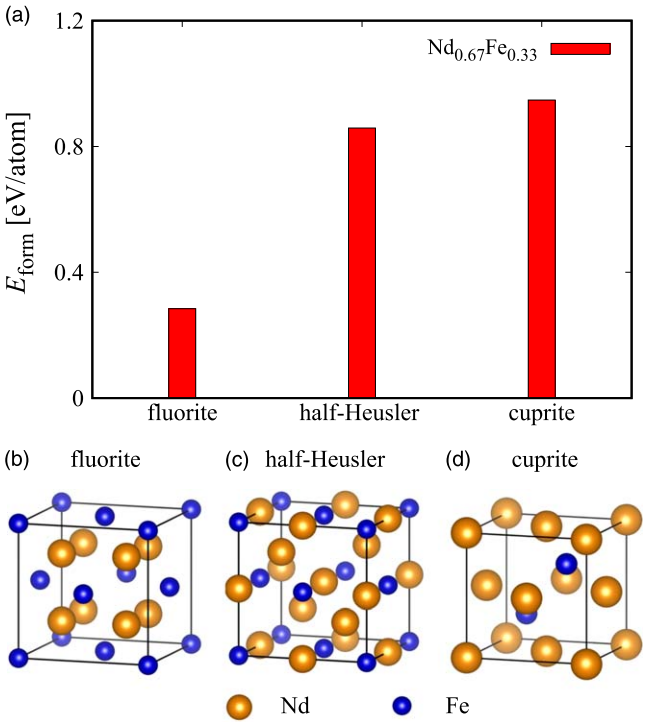

Fig. 1. (Color online) (a) Formation energies E_{form} and (b)–(d) optimized crystal structures of crystalline $Nd_{0.67}Fe_{0.33}$ alloys.

that the formation energy for $x = 1$ is remarkably high, because it has the simple cubic structure. Thus, the structural phase transition into close-packed structures of the Nd sublattice is expected for large x. In the case of decreasing x from $x = 0.67$, we examined possibilities that vacancies are formed by removing Nd atoms and Nd atoms are substituted with Fe atoms. We have found that the substitution of 8c Nd sites by Fe is more stable than the Nd-vacancy formation. In contrast with the case of increasing x, the crystal structure becomes gradually distorted as x decreases, where an example can be seen in Fig. 2(b). The fluorite-like structure is found to be kept roughly for $0.6 < x$. Under this lower limit, the alloy cannot keep its crystal structure becoming completely amorphous. This result is consistent with experimental observations, where the composition ratio of Nd in the crystalline GB phase was mainly found in a range of approximately 60–70 at%.[23] Decreasing in x from 0.67, the formation energy increases, where the slope of the curve in Fig. 2(c) is larger than that in the case of increasing in x from 0.67. This can be attributed to the fact that the structure becomes gradually distorted in the case of decreasing in x. Summarizing these two cases, the stability of the crystal structure for the fluorite Nd_xFe_{1-x} is seen for a wide composition range of approximately $0.6 < x \leqslant 1$. For this binary system, the entropy effect is necessary to stabilize the fluorite alloys, because the formation energy for this phase is always positive.

In addition to the entropy effect, a third element might promote the formation of crystalline Nd–Fe alloys. Thus, we examined ternary Nd–Fe–M compounds, where we chose M as Al, Co, Cu, and Ga. In calculating the $Nd_{0.67}Fe_{0.33-y}M_y$ alloys, we adapted a $2 \times 2 \times 2$ supercell with 96 atoms, where Fe 4a sites are replaced with M. The sites occupied by M are chosen by the SQS method. Figure 3 illustrates the

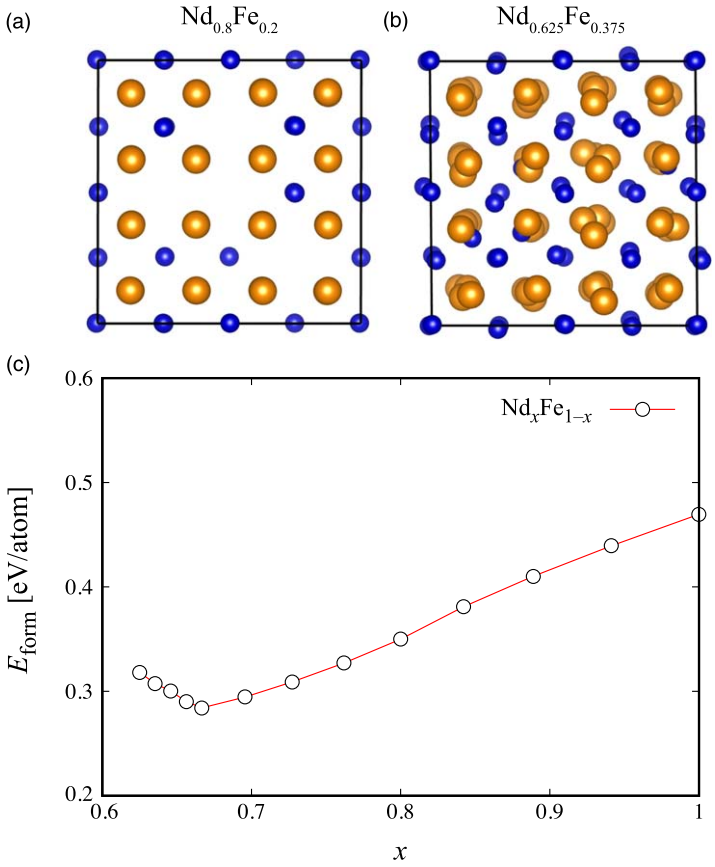

Fig. 2. (Color online) Optimized crystal structures of the fluorite Nd–Fe alloys for (a) $Nd_{0.8}Fe_{0.2}$ and (b) $Nd_{0.625}Fe_{0.375}$. (c) The formation energies E_{form} of the fluorite Nd–Fe alloys.

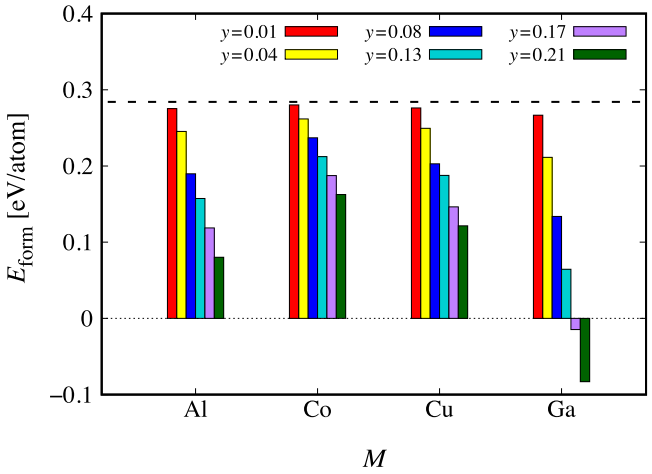

Fig. 3. (Color online) Formation energies of fluorite $Nd_{0.67}Fe_{0.33-y}M_y$ alloys. The dashed line indicates the formation energy of the binary $Nd_{0.67}Fe_{0.33}$ alloy with the fluorite structure. For $y = 0.17$, the composition should be read as $Nd_{2/3}Fe_{1/6}M_{1/6}$.

formation energies of the fluorite $Nd_{0.67}Fe_{0.33-y}M_y$ alloys ($0 \leqslant y \leqslant 0.21$). In all the cases, the formation energy is lower than the case of the binary alloy $Nd_{0.67}Fe_{0.33}$ with the fluorite structure. Furthermore, the negative formation energies of Nd–Fe–Ga alloys indicate that Ga promotes alloying compared with the other alloying elements. This stabilization by the Ga substitution comes from the interaction between Ga 4*p* states and Nd 5*d* states. The Mulliken population analysis revealed the transfer of 0.59 electrons from Nd 5*d* states to Ga 4*p* states for $y = 0.01$. Comparing the four alloying elements, we also found that the increase in the number of *p* electrons monotonically contributes to the stabilization as shown in Table II. Figure 4 shows the optimized crystal structures of the fluorite $Nd_{0.67}Fe_{0.33-y}Ga_y$ alloys. The addition of Ga does not cause structural distortions. Our result is consistent with the fact that the crystalline Nd–Fe alloys have been observed in Ga-added Nd–Fe–B permanent magnets.[24)]

Table II. Change in the number of *p* electrons Δn_p from the bulk state of the alloying element *M* for $y = 0.01$.

Element	Al	Co	Cu	Ga
Δn_p	0.11	−0.20	0.02	0.59

In contrast, the cuprite Nd_xFe_{1-x} alloys having the fcc sublattice with Nd atoms cannot keep ordered structures when Nd composition ratio deviates from $x = 0.67$, as shown in Fig. 5. The half-Heusler structure was found to be unstable for the variation of the composition as well. As already mentioned, the quasi-sphalerite and fcc Nd_xFe_{1-x} alloys cannot keep ordered structures regardless of the composition, even for $Nd_{0.67}Fe_{0.33}$ and for $Nd_{0.5}Fe_{0.5}$, where the quasi-sphalerite corresponds to the pristine sphalerite. Thus, the possibilities of cuprite, half-Heusler, fcc, and sphalerite as the crystalline Nd–Fe alloy can be excluded.

In summary, the best candidate structure for the fcc-type GB Nd–Fe phase was determined to be the fluorite structure from first-principles. This alloy Nd_xFe_{1-x} can keep its crystal structure for a wide range of the composition as $0.6 < x \leqslant 1.0$ with the minimum formation energy at

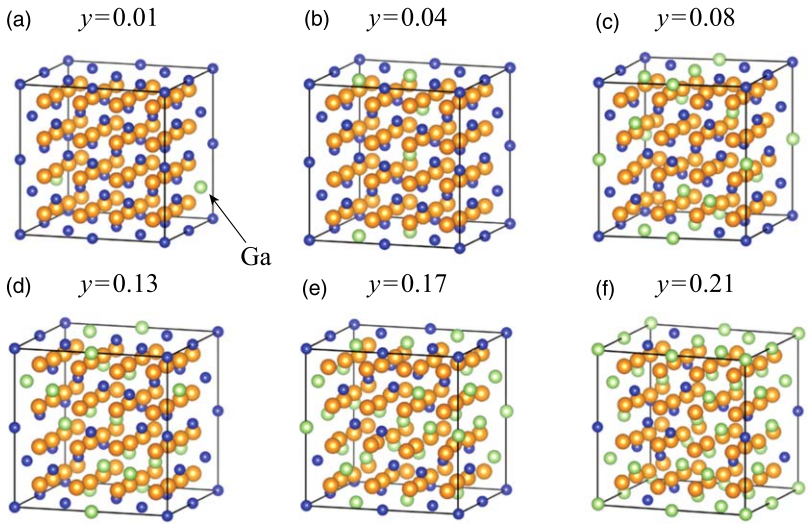

Fig. 4. (Color online) Optimized crystal structures of the fluorite $Nd_{0.67}Fe_{0.33-y}Ga_y$ alloys for (a) $y = 0.01$, (b) $y = 0.04$, (c) $y = 0.08$, (d) $y = 0.13$, (e) $y = 0.17$, and (e) $y = 0.21$. For $y = 0.17$, the composition should be read as $Nd_{2/3}Fe_{1/6}M_{1/6}$. The Fe sites occupied by Ga atoms are determined by the SQS method.

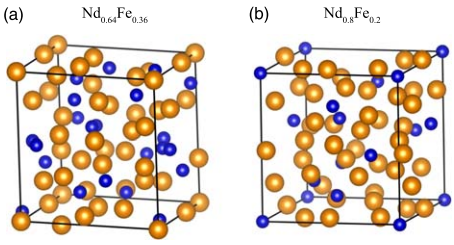

Fig. 5. (Color online) Optimized crystal structures of cuprite Nd–Fe alloys for (a) $Nd_{0.64}Fe_{0.36}$ and (b) $Nd_{0.8}Fe_{0.2}$.

$x = 0.67$. Analyzing the formation energies of Nd–Fe–*M* alloys, we conclude that adding Ga to fluorite Nd–Fe alloys can greatly promote alloying of Nd with Fe. Our new findings in this letter will hopefully trigger further understanding of the microstructure of Nd–Fe–B sintered magnets to improve the coercivity.

Acknowledgments This work was supported in part by MEXT as ESICMM Grant No. 12016013 and as a social and scientific priority issue CDMSI to be tackled by using post-K computer, and KAKENHI Grant No. 17K04978. The calculations were partly carried out by using supercomputers at ISSP, The University of Tokyo, and TSUBAME, Tokyo Institute of Technology as well as the K computer, RIKEN (Project Nos. hp180206 and hp190169).

ORCID iDs Yuta Ainai https://orcid.org/0000-0003-2741-1179 Yoshihiro Gohda https://orcid.org/0000-0002-6047-027X

1) M. Sagawa, S. Fujimura, N. Togawa, H. Yamamoto, and Y. Matsuura, J. Appl. Phys. **55**, 2083 (1984).
2) M. Sagawa, S. Fujimura, H. Yamamoto, Y. Matsuura, and K. Hiraga, IEEE Trans. Magn. **MAG-20**, 1584 (1984).
3) M. Sagawa, S. Fujimura, H. Yamamoto, Y. Matsuura, and S. Hirosawa, J. Appl. Phys. **57**, 4094 (1985).
4) D. Givord, H. S. Li, and R. Perrier de la Bâthie, Solid State Commun. **51**, 857 (1984).
5) J. F. Herbst, Rev. Mod. Phys. **63**, 819 (1991).
6) J. M. D. Coey, *Magnetism and Magnetic Materials* (Cambridge University Press, Cambridge, 2010).
7) J. M. D. Coey, Scr. Mater. **67**, 524 (2012).
8) Y. Tatetsu, Y. Harashima, T. Miyake, and Y. Gohda, Phys. Rev. Mater. **2**, 074410 (2018).
9) S. Hirosawa, J. Magn. Soc. Jpn. **39**, 85 (2015).
10) S. Sugimoto, J. Phys. D.: Appl. Phys. **44**, 064001 (2011).
11) T. Nakamura et al., Appl. Phys. Lett. **105**, 202404 (2014).
12) Y. Tatetsu, S. Tsuneyuki, and Y. Gohda, Materialia **4**, 388 (2018).
13) A. Terasawa and Y. Gohda, J. Chem. Phys. **149**, 154502 (2018).
14) N. Tsuji et al., Acta Mater. **154**, 25 (2018).
15) F. Vial, F. Joly, E. Nevalainen, M. Sagawa, K. Hiraga, and K. T. Park, J. Magn. Magn. Mater. **242–245**, 1329 (2002).
16) K. Hono and H. Sepehri-Amin, Scr. Mater. **67**, 530 (2012).
17) T. T. Sasaki, T. Ohkubo, Y. Takada, T. Sato, A. Kato, Y. Kaneko, and K. Hono, Scr. Mater. **113**, 218 (2016).
18) G. C. Hadjipanayis and A. Kim, J. Appl. Phys. **63**, 3310 (1988).
19) K. Niitsu et al., J. Alloys Compd. **752**, 220 (2018).
20) Y. Tatetsu, S. Tsuneyuki, and Y. Gohda, Phys. Rev. Appl. **6**, 064029 (2016).
21) G. Sadullahoğlua, B. Altuncevahir, and O. Addemir, Acta Phys. Pol. **125**, 1172 (2014).
22) W. F. Li, T. Ohkubo, T. Akiya, H. Kato, and K. Hono, J. Mater. Res. **24**, 413 (2009).
23) T. T. Sasaki, T. Ohkubo, and K. Hono, Acta Mater. **115**, 269 (2016).
24) X. D. Xu, T. T. Sasaki, J. N. Li, Z. J. Dong, H. Sepehri-Amin, T. H. Kim, T. Ohkubo, T. Schrefl, and K. Hono, Acta Mater. **156**, 146 (2018).
25) T. Ozaki, Phys. Rev. B **67**, 155108 (2003).
26) J. P. Perdew, K. Burke, and M. Ernzerhof, Phys. Rev. Lett. **77**, 3865 (1996).
27) A. Zunger, S. H. Wei, L. G. Ferreira, and J. E. Bernard, Phys. Rev. Lett. **65**, 353 (1990).